Universität Stuttgart

Schriftenreihe der Institute des Studiengangs Geodäsie und Geoinformatik

Technical Reports
Department of Geodesy and Geoinformatics

Y. Kuroishi

On the application of downward continuation of surface gravity onto the reference ellipsoid, to the geoid determination in mountainous areas

ISSN 0933-2839 Report Nr. 2002.2

Schriftenreihe der Institute des Studiengangs Geodäsie und Geoinformatik
Technical Reports
Department of Geodesy and Geoinformatics, Universität Stuttgart

On the application of downward continuation of surface gravity onto the reference ellipsoid, to the geoid determination in mountainous areas

Yuki KUROISHI, D. Sc.
Geographical Survey Institute
Ministry of Land, Infrastructure, and Transport
Japan
yuki@gsi.go.jp

Preface

The report was prepared by Dr. Yuki KUROISHI, while he was staying in Geodetic Institute of Stuttgart University as a Humboldt Research Fellow. The author is very much grateful to have been able to stay and work together with my dear colleagues here at Geodetic Institute. He appreciates his host professor, Prof. Dr. Erik W. Grafarend and Mrs. Ulrike Grafarend from the bottom of his heart for giving him this opportunity and taking the best cares of his family and him with hearty hospitality, which made their German stay comfortable, enjoyable, and memorable. The study was initiated as a joint work of the author and Prof. Dr. A.A. Ardalan when Prof. Ardalan was visiting the institute. The author is very grateful with the collaboration with Prof. Ardalan.

The author's thanks shall be also extended to the Alexander von Humboldt Stiftung for their support.

Abstract

Based on Ardalan (2000), the application of downward continuation of surface gravity modulus onto the reference ellipsoid to geoid determination in mountainous areas is considered as the fixed-free two-boundary value problem. Supposed that surface gravity data have good coverage, the question is discussed if the system of equations be ill-posed and some regularization be required. In the application of Abel-Poisson integral, modifications to the kernel and its computation for the discrete data are proposed to adapt a case of dense coverage. Necessity becomes clear that we must develop some physical reductions to suppress (smooth) the variations of incremental gravity modulus in mountainous areas.

1. Introduction

The geoid determination is one of the most fundamental problems in geodesy. Space geodetic techniques such as GPS (the Global Positioning System) easily provide accurate three-dimensional positions at the Earth surface, which yield the ellipsoidal heights with accuracy of cm- or even of mm- order. The techniques necessitate a precise model of the geoid in the practical world (engineering survey) as well as in the geodetic community. The techniques also provide us the opportunity to apply the fixed-boundary value or fixed-free two-boundary value problem such that gravity observables on the known boundary of the Earth surface are used to determine the position of the unknown boundary of the geoid.

In this context, Ardalan (2000) proposed one such methodology in a remove-restore manner. Gravity moduli by gravimetry and/or geopotential numbers by precise leveling and gravimetry are given at the Earth surface known by GPS measurements. A global geopotential model complete up to 360 degrees and orders, and the centrifugal potential are removed from the observation data. The effects of the local topographic masses are also computed and removed from the data to prepare the incremental signals in the harmonic space down to the reference ellipsoid. The downward continuation is applied to the incremental signals for yielding the incremental potentials at the reference ellipsoid. The contributions of the global geopotential model, centrifugal potential and local topographic masses to the geopotential are restored at this level and the geoid heights are given by the Bruns' formula.

The methodology is not well evaluated in terms of the applicability to the actual data of different areas in different geological conditions. One of the difficulties to apply the fixed-free two-boundary value problem is that required data, gravity or geopotential num

ber data, are not yet given densely. On the contrary, there are many areas where dense surface gravity data without three-dimensional (geocentric) position information are available.

In this paper, the methodology is tested with surface gravity data in the most mountainous area of Japan, which includes Mt. Fuji and Southern Japanese Alps, (hereinafter we refer to the area as 'Fuji area') and some modifications/improvements are given to the methodology. We apply the downward continuation only of gravity modulus in the test. We put emphases on the following questions:

- Is the downward continuation in this case really ill conditioned and is some type of regularization really required?
- How should we handle the singularity of modified Abel-Poisson kernel in the numerical computation with discrete data?
- Is the proposed methodology applicable to the real data in mountainous areas? That is, are the incremental potentials on the reference ellipsoid smooth? (That condition is presumed in the downward continuation with the kernel dumping rapidly near the origin.)

As already mentioned in the proceeding paragraph, we do not actually have the three-dimensional positions for the gravity data in Fuji area. Here, we use the latest gravimetric geoid model for Japan, JGEOID2000 (Kuroishi, 2001) on a 1 by 1.5 arc-minute grid to convert Helmert orthometric heights to the ellipsoidal heights. Kuroishi (2001) showed that the errors of JGEOID2000 are in a range of a few tens of centimeters over Fuji area in comparison to the nationwide net of GPS at benchmarks. The neglect of the errors may not yield any significant errors in the resulting geoid model.

2. Area of Study

Fuji area is selected for the study. The area includes the highest peak of Japan, Mt. Fuji and some mountain ranges whose elevations exceed 3 000 m. The topography is shown in Fig.1. The geoid computation is made with gravity data distributed in the area of 35°10′-36°N by 137°45′-139°E in the local reference frame (Tokyo Datum).

The surface gravity data have a good coverage around Mt. Fuji, but have some data gaps in mountain ranges. The existence of data gaps makes us possible to evaluate their effects in the downward continuation computation.

We set a data cell of 1 by 1.5 arc-minute, which is a compatible resolution with that of JGEOID2000, and check the data distribution. If there exist more than two data in a cell, we remove such data except the one nearest to the center of the cell. By this process we can make the distribution of used data close to homogenous one. The final distribution of the surface gravity data is shown in Fig. 2.

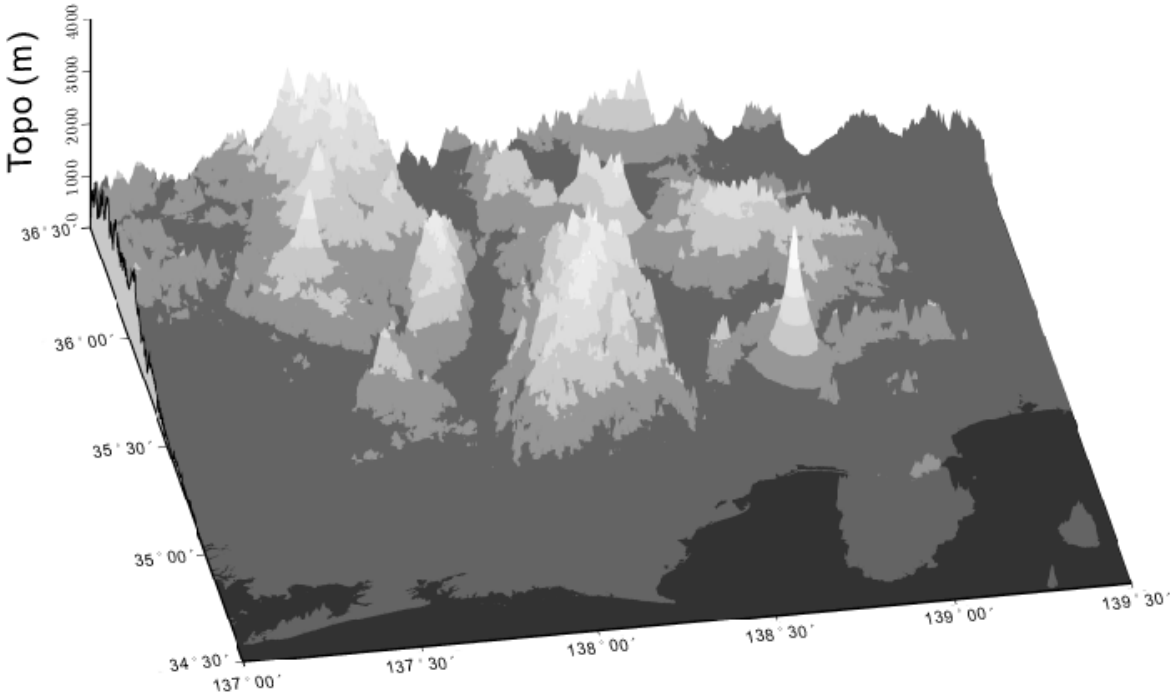

Figure 1: Bird's eye view of topography in Fuji area. Black area shows Pacific Ocean.

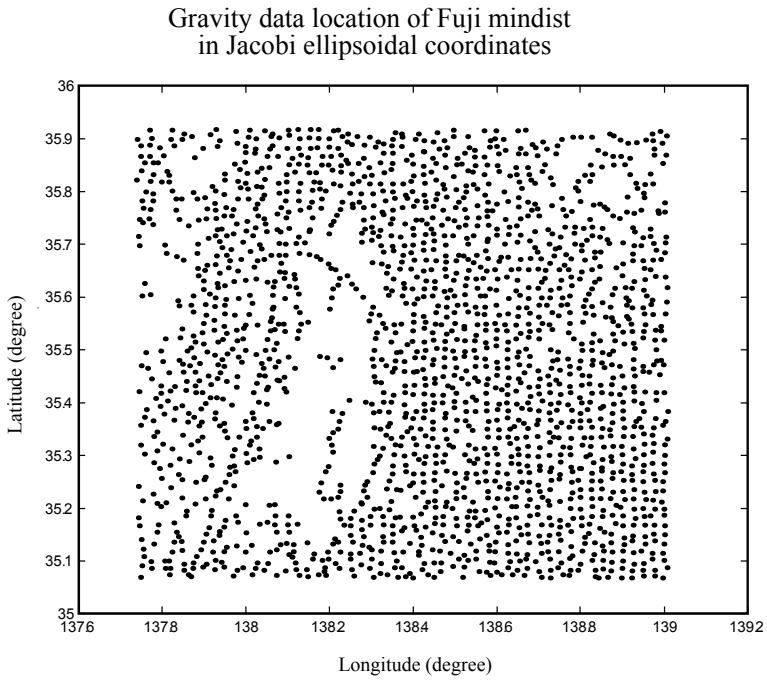

Figure 2: Distribution of surface gravity data in Fuji area.

In the numerical computation of downward continuation, we must have data redundancy in terms of least squares adjustment. In this study, we set a computational grid of 2 by 3 arc-minutes on the reference ellipsoid.

3. Corrections and modifications to the preceding study by Ardalan (2000)

In order to make the points of discussion clear, we summarize the corrections and modifications made to the preceding study by Ardalan (2000).

Proposed Corrections and modifications to Ardalan (2000)

1) Formula (1.85) for the area of the reference ellipsoid:
The original formula,

$$S=4\pi a\left\{\frac{1}{2}+\frac{b^2}{4a\varepsilon}\ln\frac{a+\varepsilon}{a-\varepsilon}\right\}$$

should be corrected as follows:

$$S=4\pi a^2\left\{\frac{1}{2}+\frac{b^2}{4a\varepsilon}\ln\frac{a+\varepsilon}{a-\varepsilon}\right\}$$

The correction is a factor of a^{-1} to the right-hand side of the equation of downward continuation. Due to this error, the computed downward-continued incremental potentials at the ellipsoid were by far small and showed almost no significant signals in the resulting maps in Figs. 2-19 and Figs. 2-35 of Ardalan (2000) but spike noises. The correction can be confirmed by checking some books of mathematical formula library or by thinking of the unit dimension of the right-hand side. The area should have a unit of squared lengths.

2) Corrections to the sign of the restored contribution of the local topographic masses:
In page 108 of Ardalan (2000), the negative sign is assigned to the restoration term. There is no reason to reverse the sign of the potential computation. The resulting geoid models in Figs. 2-41 and 2-43 of Ardalan (2000) show the significant disagreement against EGG97 (Fig. 2-28) in the southwestern part, where the Ardalan's geoid models have a dented pattern due to the opposite corrections of the local topographic mass contribution (Fig. 2-22). Since EGG97 model matches pretty well with GPS/leveling-derived geoid undulations (height anomalies), the dented pattern indicates the sign mistake.

3) Modifications to the Modified Abel-Poisson kernel:
Ardalan (2000) employs the removal of the zero-degree term and the degree 1/order 0 term. In the methodology, we should not correct the degree-zero (corresponding to the geocentric mass) or the degree-one terms (corresponding to the coincidence of the mass center with the ellipsoidal origin). Then, we additionally remove the degree 1/order 1 and – 1 terms.
Those are given as follows:

$$K_{1,-1}+K_{1,1}=\frac{3Q^*_{1,1}(\sinh\eta)}{Q^*_{1,1}(\sinh\eta_0)}\cos\phi\cos\phi'\cos(\lambda-\lambda')$$

$$\frac{\partial(K_{1,-1}+K_{1,1})}{\partial\lambda}=-\frac{3Q^*_{1,1}(\sinh\eta)}{Q^*_{1,1}(\sinh\eta_0)}\cos\phi\cos\phi'\sin(\lambda-\lambda')$$

$$\frac{\partial(K_{1,-1}+K_{1,1})}{\partial\phi}=-\frac{3Q^*_{1,1}(\sinh\eta)}{Q^*_{1,1}(\sinh\eta_0)}\sin\phi\cos\phi'\cos(\lambda-\lambda')$$

$$\frac{\partial(K_{1,-1}+K_{1,1})}{\partial\eta}=\frac{3\cos\phi\cos\phi'\cos(\lambda-\lambda')}{Q^*_{1,1}(\sinh\eta_0)}\left\{1+\frac{1}{\cosh^2\eta}-\sinh\eta\cot^{-1}(\sinh\eta)\right\}$$

4) Removal of regularization procedures in the downward continuation in the case of densely covered data, instead some grid points, with a certain criterion in terms of the distance of the nearest data, are removed in the computation:

5) Modifications to the numerical computation of downward continuation in the innermost cell, that is the modification to the kernel computation algorithm:
The modified Abel-Poisson kernel is given as follows:

$$K(\lambda,\phi,\eta;\lambda',\phi',\eta_0)=K_{spherical}-K_{0,0}-K_{1,1}-K_{1,-1}-K_{1,0}$$

$$K_{spherical}=R\frac{r^2-R^2}{\|\vec{x}-\vec{x}'\|^2}$$

$$\vec{x}\equiv(\lambda',\phi',\eta_0),\ \mathrm{R}\equiv\|\vec{x}\|$$

$$\vec{x}'\equiv(\lambda,\phi,\eta),\quad \mathrm{r}\equiv\|\vec{x}'\|$$

$$K=R\left\{\frac{r^2-R^2}{\|\vec{x}-\vec{x}'\|^2}\frac{1}{r}-\frac{3R}{r^2}\cos\psi\right\}\ \text{in the spherical expression}$$

where ψ is the spherical distance between the points, $\vec{x}$ and $\vec{x}'$

The integration of the $K_{spherical}$ term with an infinitesimal area element at the ellipsoid has no singularity in the analytical form. But in the discrete procedure, the computation of this term becomes singular at the origin. In the procedure, we set regular cells with a finite area and replace the integral of each cell contribution by the multiplication of the incremental potential (treated constant over the cell) with the kernel value at the cell center. Then the computation becomes unstable (provides anomalous results) where the computation point sits very close to the surface data point.

Only the $K_{spherical}$ term shows in the employed discrete computation a singularity at the point where the computation point coincides with the data point. But in the numerical computation, we compute each term at the grid point with a certain finite size of cell. What do we actually compute the terms? In the discrete computation, we treat that incremental potentials at the ellipsoid are given in a step-wise distribution, meaning that the potentials are equal over each cell. The contribution of the potential of each cell element to the Earth surface gravity is computed by multiplying the poten

tial by the modified Abel-Poisson kernel, which is computed only from the positions of the gravity data and the cell center (grid). We should note that we do not really compute the contribution by integration.

The computed contributions should be correct only when the average of the modified kernel values in the cell is equal to the value computed at the cell center. This is true if the kernel function is close to the bilinear surface. And this would be the case with the cells except the innermost one. For the innermost cell whose center falls very close to the data point, the computed value of the modified Abel-Poisson kernel or its gradient changes drastically in association with small changes of the computation positions. Then the computed contributions can be by far away from the correct ones.

In this study we change the computation algorithm for the contribution of the innermost cell. The original formula for the gravity modulus is given as (1.140) in Ardalan (2000). Since the area of the innermost cell is very small, we can compute the integral over the cell under a planar approximation and the cell can be replaced by the planar circle of the same area. In addition, we can evaluate only the component normal to the ellipsoid, because the contribution of the innermost cell to the incremental gravity vector on the topography is mapped with the reference gravity vector and the reference gravity vector can be assumed parallel to the ellipsoidal normal.

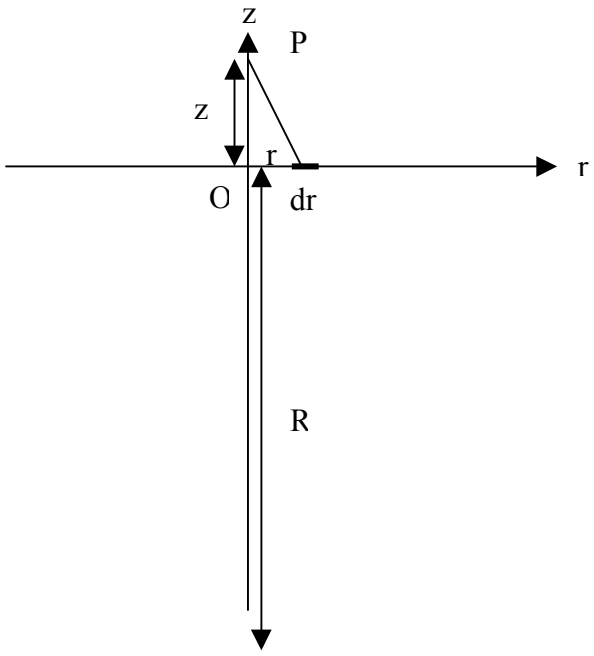

Figure 3: Coordinate system for downward continuation of incremental potential of innermost cell under planar approximation. Solid line shows the area element of the cell and *P* is the position at the topographic surface. *R* is the mean radius of the Earth, *r* is the surface distance between the projected point of *P* to the ellipsoid and the element center, and *z* is the height of point *P*.

In the planar approximation, the contribution of the potential in the innermost cell of the radius r_0, can be computed, in the coordinate system given in Fig. 3, as follows:

$$\delta g_P^{inn} = \frac{\Gamma_z}{\|\vec{\Gamma}\|}\frac{1}{4\pi R}\iint_{d\sigma}\frac{\partial K}{\partial z}V_{inn}\,d\sigma$$

$$= \frac{\Gamma_z}{\|\vec{\Gamma}\|}\frac{V_{inn}}{4\pi R}\int_0^{2\pi} d\alpha \int_0^{r_0} r dr \frac{\partial K}{\partial z}$$

$$\frac{\partial K}{\partial z} = \frac{-\left(z^3+4Rz^2\right)+2\left(R+z\right)r^2}{\left(z^2+r^2\right)^{5/2}} + \frac{7R+z}{\left(R+z\right)^3} - \frac{3r^2}{\left(R+z\right)^3 R}$$

$$\therefore \delta g_P^{inn} = \frac{\Gamma_z V_{inn}}{\|\vec{\Gamma}\|}\left[\frac{6r_0^5+5z^3\left(z^2+r_0^2\right)-15z\left(z^2+r_0^2\right)^2}{15z\left(z^2+r_0^2\right)^{5/2}} + \frac{1}{2R}\left(\frac{7r_0^2}{2R^2}-\frac{3r_0^4}{4R^4}\right)\right]$$

where V_{inn} is the constant (incremental) potential in the innermost cell, R is the geocentric radius of the innermost cell, z is the height of the surface point P where the incremental gravity, δg_P should be computed. In the last bracket of the last equation, $R \gg z$ is assumed. In the derivation, the point P is assumed to be on the ellipsoidal normal at the cell center.

The computation should be made in Jacobi's ellipsoidal coordinates. The parameters, R, z, and r_0 can be given as follows:

$$R = a\sqrt{\frac{1}{2}+\frac{b^2}{4a\varepsilon}\ln\frac{a+\varepsilon}{a-\varepsilon}}$$

$$z = \varepsilon\sqrt{1-e^2}\sinh\eta\cos\phi\sqrt{1+\frac{\tan^2\phi}{1-e^2}} - \frac{a\left(1-e^2\right)}{\sqrt{1-\dfrac{e^2\tan^2\phi}{1-e^2+\tan^2\phi}}}$$

$$r_0 = R\sqrt{\frac{\cos\phi'\Delta\phi\Delta\lambda}{\pi}}$$

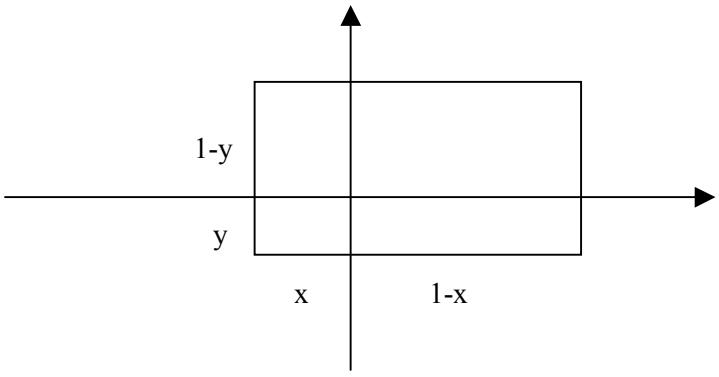

Figure 4: Position of surface point P with respect to center of innermost cell in an eccentric case. The point P is the coordinate origin and the square shows the relative position of the innermost cell. The relative areas in each quadrant are given by the two numbers, x and y ($0 \leqq x \leqq 1$, $0 \leqq y \leqq 1$).

In real cases, the point P may not be on the ellipsoidal normal. In order to evaluate the contribution in general situations, we set a two-dimensional position of the point

P eccentric with respect to the cell center as shown in Fig. 4. The areas of the inner-most-cell sections in the first, second, third, and fourth quadrants relative to the total area can be given as follows:

$$S_1 \equiv (1-x)(1-y)S = \frac{1}{4}\pi r_1^2$$

$$S_2 \equiv x(1-y)S = \frac{1}{4}\pi r_2^2$$

$$S_3 \equiv xyS = \frac{1}{4}\pi r_3^2$$

$$S_4 \equiv (1-x)yS = \frac{1}{4}\pi r_4^2$$

$$S \equiv \pi r_0^2 = S_1 + S_2 + S_3 + S_4$$

$$\therefore r_1^2 = 2r_0^2(1-x)(1-y)$$

$$\therefore r_2^2 = 2r_0^2 x(1-y)$$

$$\therefore r_3^2 = 2r_0^2 xy$$

$$\therefore r_4^2 = 2r_0^2(1-x)y$$

The contribution of each quadrant can be computed by the same formula with the corresponding radius r_1, r_2, r_3, and r_4 divided by 4. In this paper, we simply use the computational result obtained only with r_0.

4. Spatial pattern of the newly modified Abel-Poisson Kernel

The spatial shapes of the first partial-derivatives of the newly modified Abel-Poisson Kernel are shown in Fig. 5 (a), (b), and (c) for the longitudinal, latitudinal, and eta components, respectively. The figures exhibit sharp dumping of all partial derivatives in each direction. The major powers, as a response function to the incremental potential at the ellipsoid, are concentrated in the central area within a radius of, say, 4-5 arc-minutes.

We must get the meaning of the methodology, i.e. the numerical computation of downward continuation, from the spatial characteristics. The incremental gravity data just around the computational points, on the ellipsoid, within such a radius heavily control the incremental potentials at the ellipsoid. In the case that some computational cells on the ellipsoid do not have any data within the sufficient distance, the normal matrix of the least squares equation becomes weak at such cells. In addition, the geoid determination by the proposed methodology is applied to discrete data. The resulting geoid models shall badly oscillate depending on the available data, in such a case that the incremental gravity field at the topographic surface be not smooth and that the actual data distribution be neither dense nor homogenous.

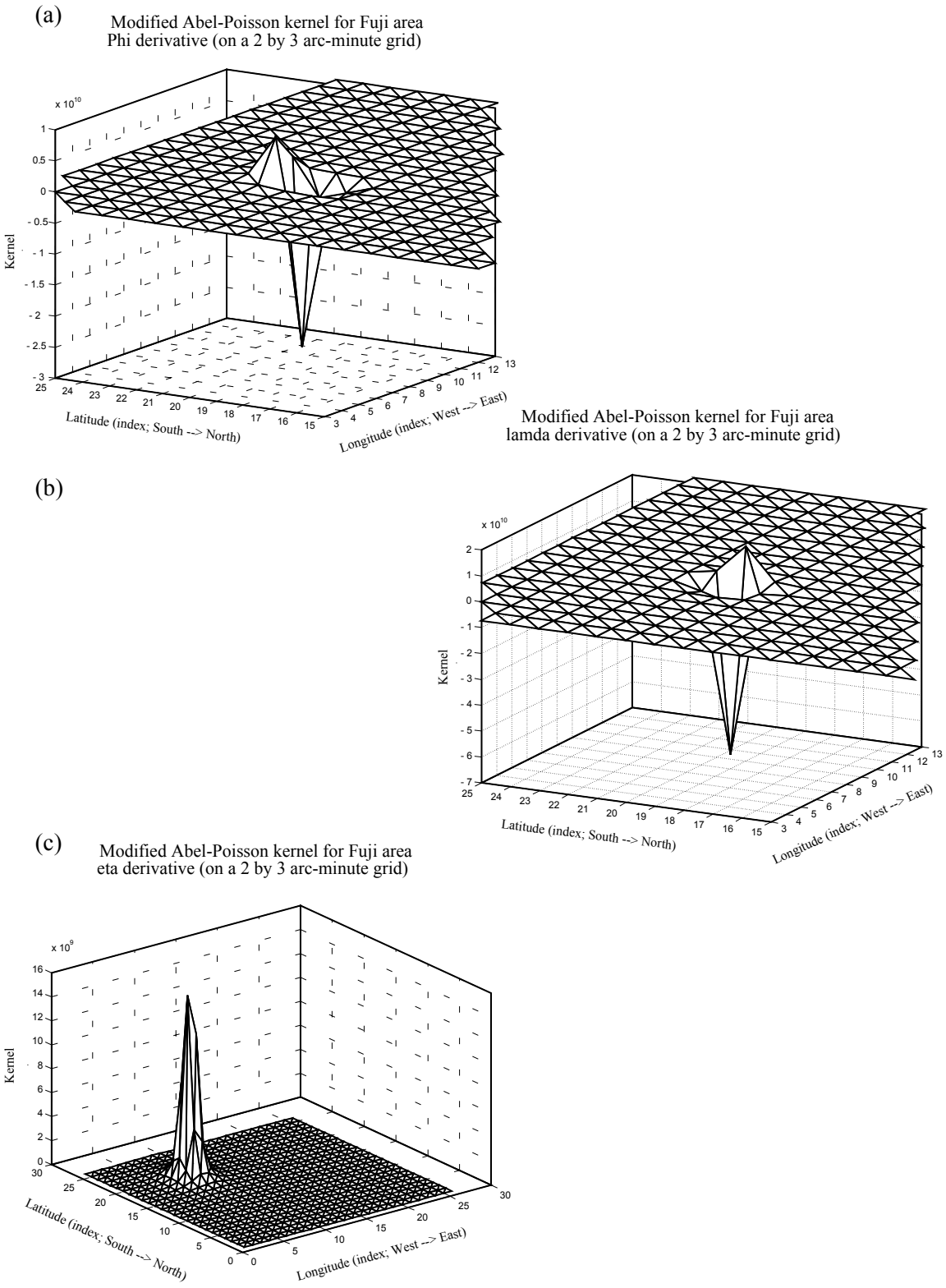

Figure 5: Spatial pattern of gradient of Modified Abel-Poisson kernel: (a) latitudinal (phi) component, (b) longitudinal (lamda) component, and (c) height (η) component. The computation of the kernel is made only at the lattice points shown with solid lines and the intervals are 2 arc-minutes and 3 arc-minutes in latitudinal and longitudinal directions, respectively.

The downward continuation problem of the gravity field (anomalies) is ill-conditioned in the case that the satellite-altitude data are continued down to the ellipsoidal or topographic surfaces. This phenomenon comes from the higher-degree harmonics having controlling terms of $(1+h/R)^{n+1}$ or alike. In the satellites' altitudes, the magnitude of h/R is not small enough and the higher-degree terms enhanced by factor (n+1)h/R become too big, which yields the ill-posedness. But as discussed in Martinez (1998), the downward continuation from the topographic surface to the ellipsoidal surface is not ill-posed by itself.

In Fuji area, there are some data gaps in some mountainous areas. Because of the too-high sensitivity of the response function (the first derivatives of the modified Abel-Poisson kernel) to the near-zone data, the system equations of the least squares adjustment show weakness in such data gap areas when we set a regular fine-grid on the ellipsoid for computation. We estimate the errors of the incremental potentials on the computational grid of 2 by 3 minutes and show their spatial pattern in Fig. 6. An area of big errors is located in the southeast part, which clearly corresponds to the data gaps shown in Fig. 2. Then, we exclude the points from which no surface gravity data exists within a certain distance. The distance should be a critical radius and we use the value of 3 arc-minutes as a test. The distribution of the remaining points of computation is shown in Fig. 7. As a result, only three points are removed.

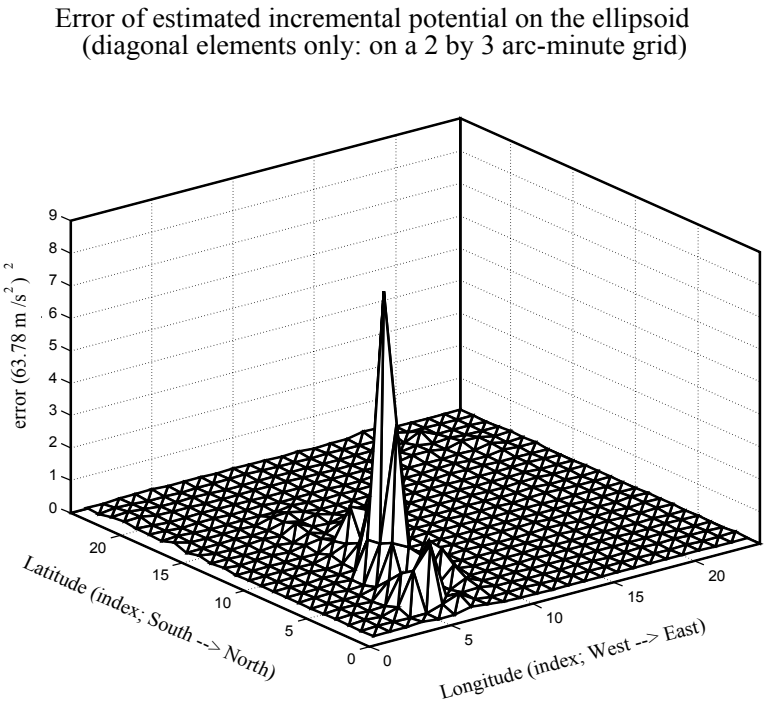

Figure 6: Spatial distribution of error of downward-continued incremental potentials on ellipsoid, estimated by least squares adjustment. Note that the unit of the vertical axis is 63.78 m^2/s^2.

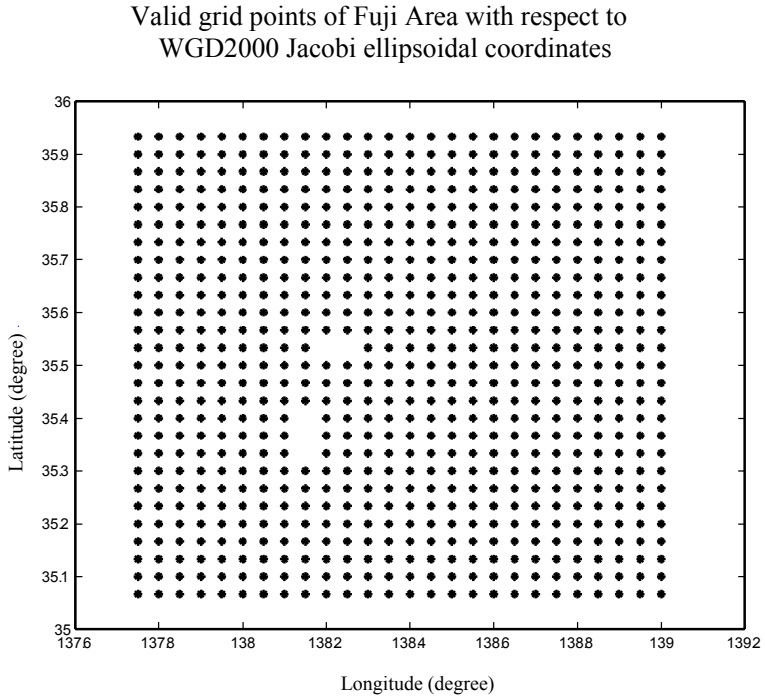

Figure 7: Location of computation points on ellipsoid, used in the study. The critical radius is set at 3 arc-minutes.

5. Computation of contribution of incremental potential in innermost cell to surface gravity modulus

As we discussed in the section 3, we changed the algorithm for the computation of the first derivatives of the modified Abel-Poisson kernel for the innermost cell. The differences of the eta-components between the two algorithms are computed for the data of Fuji area and those of 100 randomly sampled surface gravity data are shown in Fig. 8. The values computed using the new algorithm distribute smoothly, but the corresponding values computed using the old algorithm show a big scatter at some points, whose values differ by more than order of 2.

The corresponding elements of the design matrix of downward continuation in the least squares adjustment are also calculated and shown in Fig. 9. The elements show a smooth distribution in the case with the new algorithm, but a scatter again in the case with the old algorithm. The errors associated with the old algorithm should yield significant distortion in the results on such an order.

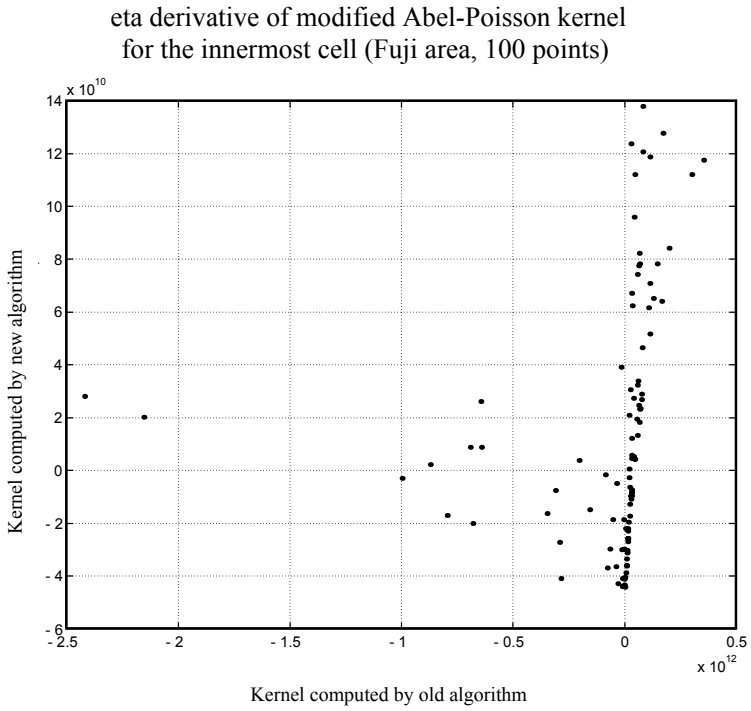

Figure 8: Comparisons of eta component of first derivatives of modified Abel-Poisson kernel between the old, point-wise computation (Ardalan, 2000) and the new, integration computation. Only 100 points are selected for plotting. The horizontal and vertical axes give the results by the former and latter algorithms, respectively.

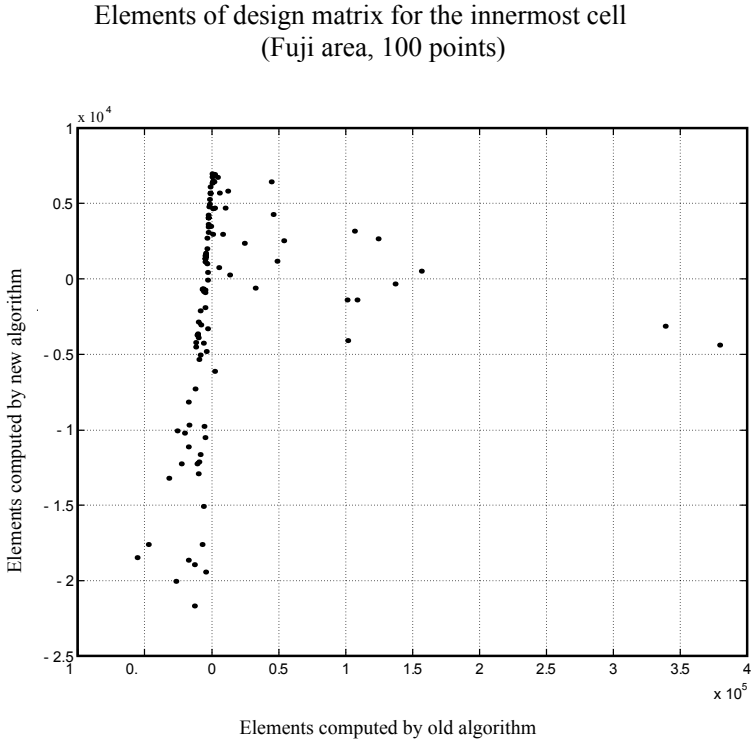

Figure 9: Comparisons of elements of design matrix of downward continuation for innermost cell, between the old, and new algorithm. The same 100 points as those shown in Fig. 8 are evaluated.

6. Results of geoid determination by downward continuation

6.1 Incremental surface gravity modulus

The solutions of downward continuation are computed with the discussed data and methodology. Effects of local topographic masses within the distance of 50 km are computed with a digital elevation (orthometric height) model (DEM) on a 7.5 by 11.25 arc-second grid. The DEM is given on a regular grid in the reference frame of Tokyo Datum. The removal and restoration of the effects are evaluated under a planar approximation, in Tokyo datum. Strictly, we should compute the effects in terms of ellipsoidal heights, but we use here the orthometric heights as the ellipsoidal heights: the geoid heights are not corrected to the DEM and the topographic masses above the geoid are removed/restored instead of those above the reference ellipsoid. The ellipsoidal heights are replaced by the orthometric heights only in the computation of the local topographic mass effects, and the ellipsoidal heights are used in the other computations such as downward continuation. The some systematic biases may yield in the removal procedures, but no significant errors will be included at medium or short wavelengths. This is because the area of the local masses is small and the variations of geoid heights within the area are also small. Additionally, major portions of the biases, if any, are cancelled in the restoration stage.

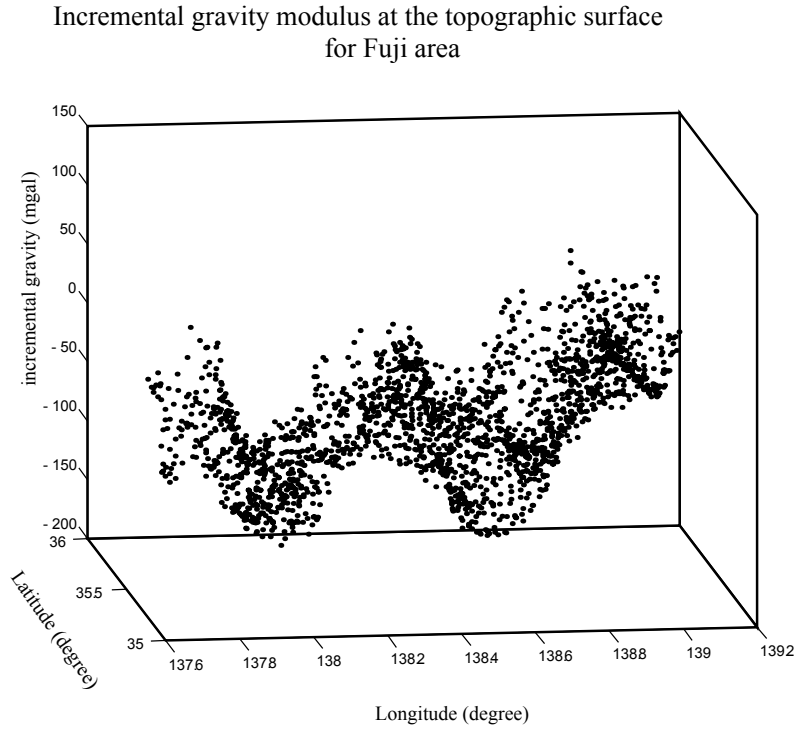

Figure 10: Geographical distribution of incremental gravity modulus at topographic surface. The incremental gravity modulus is computed by removing the effects of EGM96 global geopotential model complete to degree/order 360, centrifugal potential, and local topographic potential over distances up to 50 km.

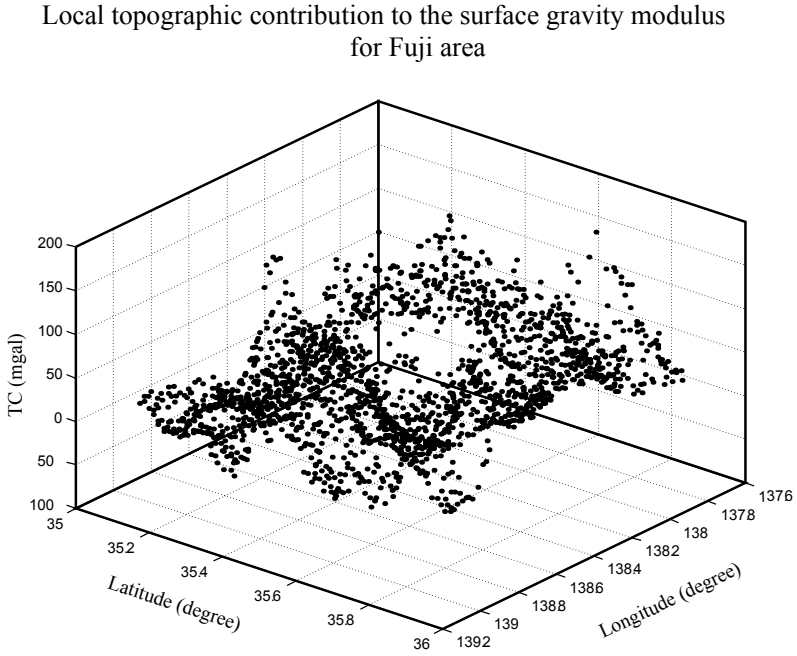

Figure 11: Geographical distribution of local topographic contribution to surface gravity modulus. Local topographic masses over distances up to 50 km are considered and denoted as TC.

The geographical distribution of incremental gravity modulus is shown in Fig. 10. The corresponding distribution of the modulus of the local topographic mass reduction (hereinafter called TC) is given in Fig. 11. As a matter of fact, the incremental gravity modulus at the topographic surface is not smooth and still contains a magnitude of undulations similar to TCs.

To look into the characteristics of the signals and reductions, we check the relations between them. We plot TCs against height in Fig. 12. TC ranges from about –70 to + 200 mgal and shows a strong, linear relation to height with short wavelength variations. It is plotted in Fig. 13 against intermediate incremental surface gravity modulus, in which only the contributions of EGM96 and centrifugal potentials are removed. The data show a linear relation with a large scatter. The intermediate incremental modulus is plotted in Fig. 14 against incremental surface gravity modulus. By the reduction of local topographic masses, the incremental surface gravity modulus shows no clear correlation with TC and still holds a big scatter in a range of –160 to + 100 mgal. The results tell us clearly that the local topographic reductions do not effectively smooth the data, contrary to our expectation. Therefore, we cannot expect that the downward continuation approach yield stable solutions to the discrete data in mountainous areas.

The incremental gravity modulus is plotted in Fig. 15 against height. It seems that the modulus still show a week dependency on height.

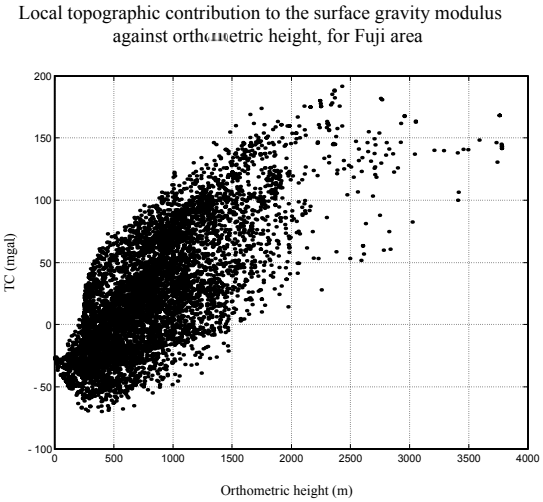

Figure 12: Local topographic contribution to surface gravity modulus against orthometric height

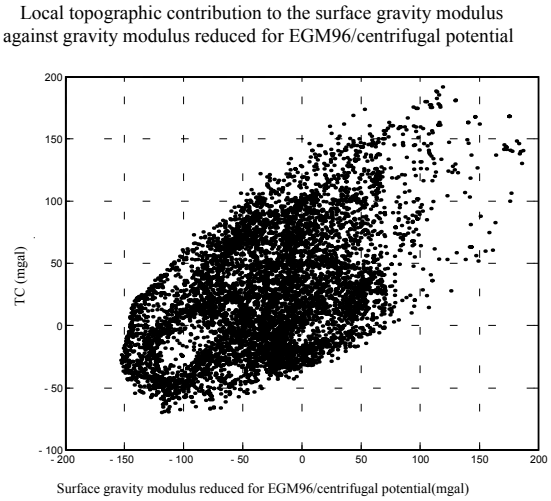

Figure 13: Local topographic contribution to surface gravity modulus against surface gravity modulus reduced for EGM96 and centrifugal potentials.

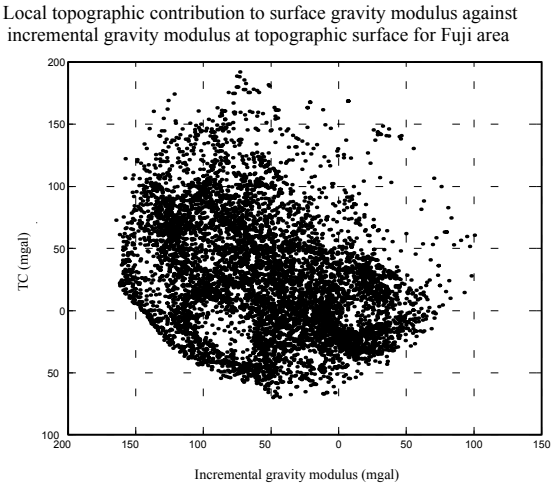

Figure 14: Local topographic contribution to surface gravity modulus against incremental gravity modulus at topographic surface.

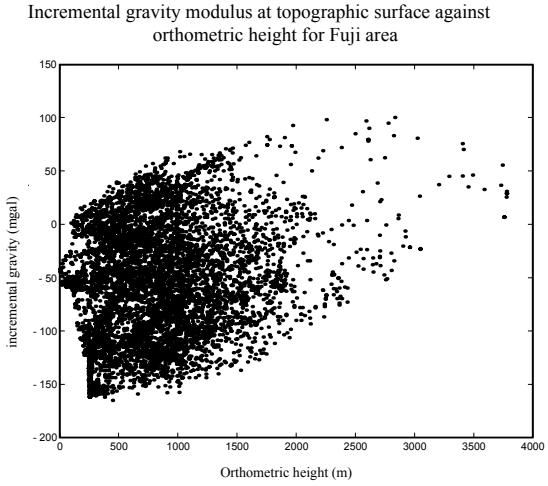

Figure 15: Incremental gravity modulus at topographic surface against orthometric height.

We should think of the reduction of local topographic masses carefully. The contribution of local topographic masses over distances up to 50 km, to the gravity modulus at the topographic surface is very close to the conventional terrain-corrected Bouguer correction. As Hagiwara (1975) showed, the contribution of a spherical shell in a cap of 0.1 to 10 arc-degrees can be expressed by the same term as that of the conventional Bouguer plate. Then the incremental gravity modulus at the topographic surface differs by the amount of the differences between the EGM96-induced and the (WGD2000) normal gravity field. In such a small area as of 50 km range, the differences are not significant and, therefore, the incremental gravity modulus is not so smooth as expected. To apply a

downward continuation approach to the geoid determination for mountainous areas, consideration of density variations in the crust and/or compensation surfaces such as Moho and Conrad discontinuities will be needed to substantially smooth the incremental signals.

6.2 Downward continuation of incremental surface gravity modulus to reference ellipsoid

Downward continuation computation is made to the prepared data of incremental surface gravity modulus. The condition number of the normal matrix without any regularization is 4.2×10^7 and the system of equations is not ill-posed as expected. The statistics of the input data, incremental surface gravity modulus, are as follows:

Average = - 61.9, Max= 100.2, Min= - 161.3, SD= 49.7 in mgal

The sigma, SD of the residuals, is 28.0 mgal. Forty-four percent of the signals are explained by the downward-continued incremental potentials.

The geographical distribution of the estimated incremental potentials on the reference ellipsoid, WGD2000 (Grafarend and Ardalan, 1999) is shown in Fig. 16. Several outliers (spike-like points) are found in some area. The grid points at which the modulus of the estimated incremental potentials exceeds 50 m^2/s^2 are plotted in Fig. 17. Comparing with Fig. 2, we recognize that these points are located in the data gap areas. This suggests that the employed critical distance of 3 arc-minutes for the exclusion from computation is a little too small.

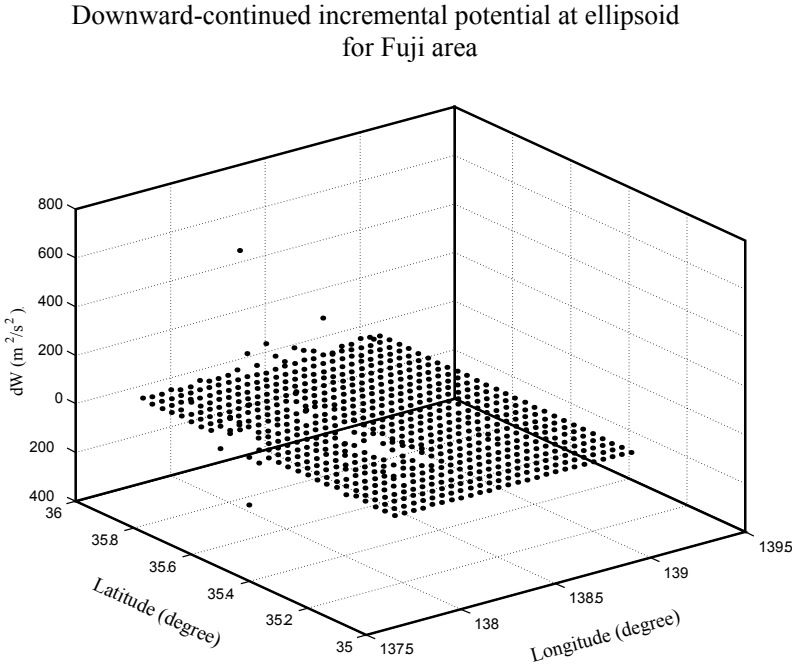

Figure 16: Geographical distribution of downward-continued incremental potential at WGD2000 ellipsoid.

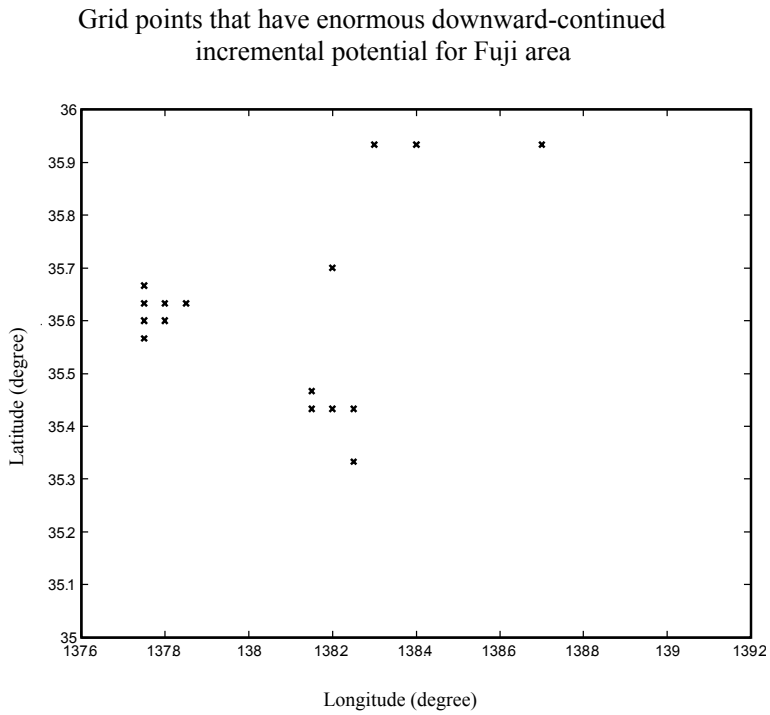

Figure 17: Location of grid points that have enormous downward-continued incremental potential, namely the potential exceeds 50 m^2/s^2.

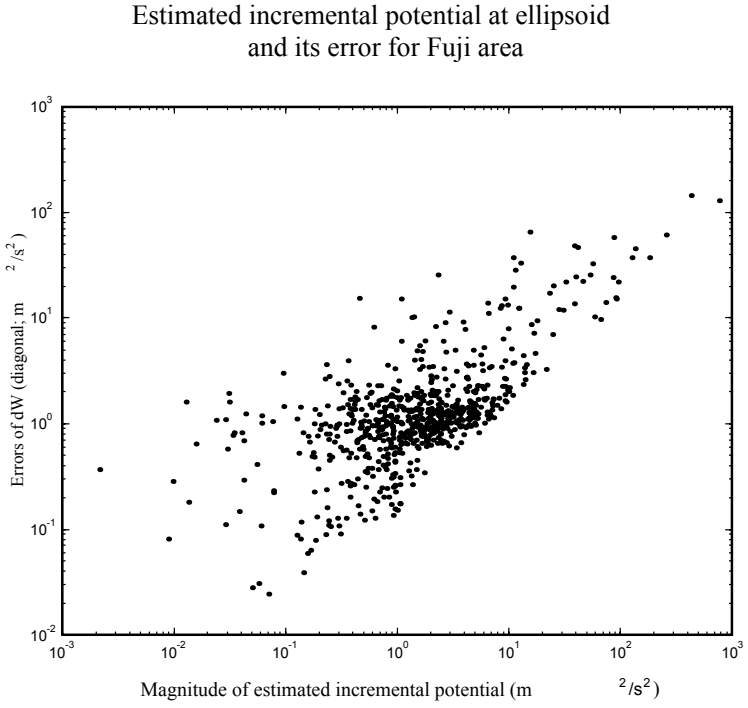

Figure 18: Estimated incremental potential at ellipsoid and its error.

The relation between the estimated incremental potentials and their errors are shown in Fig. 18. Such a general tendency is found that the points whose moduli of the estimated incremental potentials are big are accompanied by big errors.

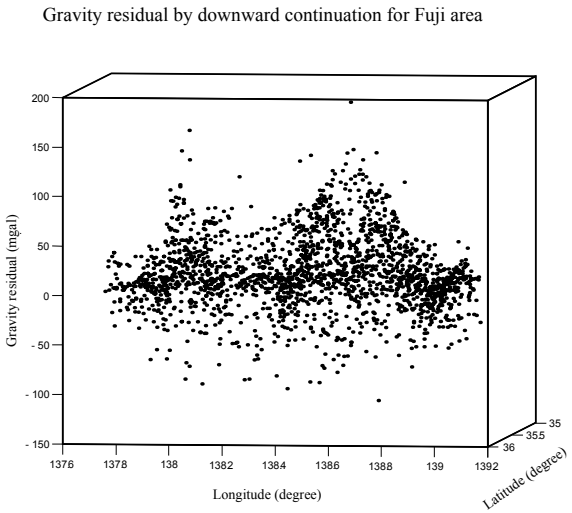

Figure 19: Geographical distribution of gravity modulus residual by downward continuation.

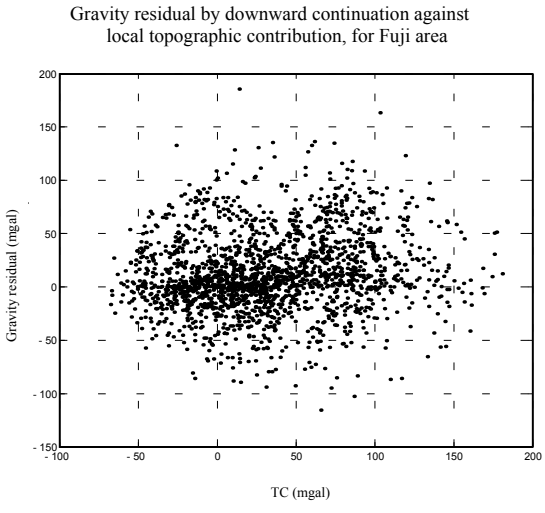

Figure 20: Gravity modulus residual by downward continuation against local topographic contribution to surface gravity modulus.

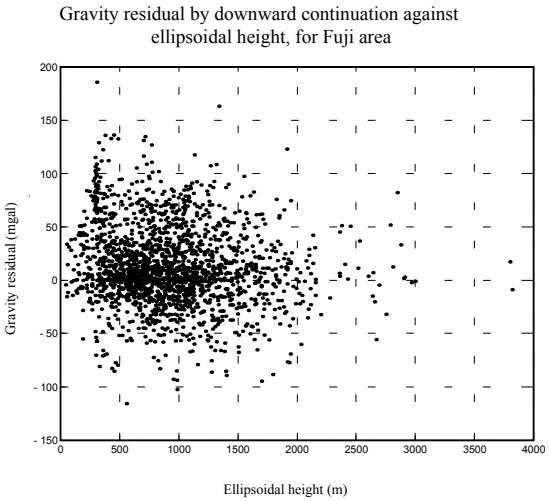

Figure 21: Gravity modulus residual by downward continuation against ellipsoidal height.

The geographical distribution of the gravity residuals after downward continuation is shown in Fig. 19. The residuals show a big scatter at short wavelengths. The gravity residuals are plotted against TC in Fig. 20 and against (ellipsoidal) height in Fig. 21. No clear dependency is observed in both figures. The non-smoothness of the input signals should result in these results.

6.3 Contributions of each restoration terms to geoid undulations

The restored, combined contributions of the EGM96 geopotential model and centrifugal potentials are computed and their geographical distribution is shown in Fig. 22. The

contributions produce the major features of geoid undulations in a magnitude of about 10 m. The restored local topographic potentials on the WGD2000 ellipsoid are illustrated in Fig. 23. The figure indicates that the local topography could produce the geoidal undulations up to 8 m and also that the contributions do not contain large signals at short wavelengths.

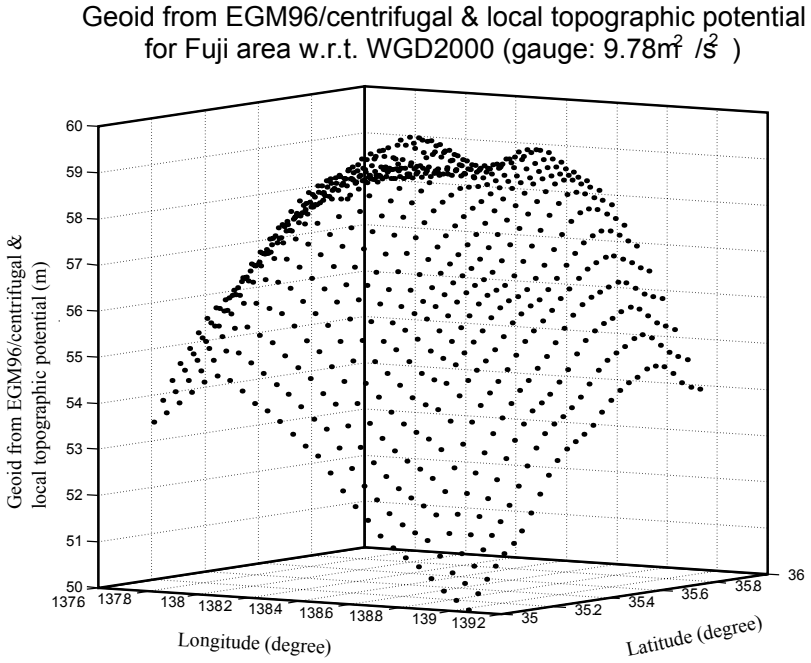

Figure 22: Geoid from EGM96, centrifugal, and local topographic potential at WGD2000 ellipsoid. The potentials are gauged by the value of 9.78 m^2/s^2 to convert into geoid heights.

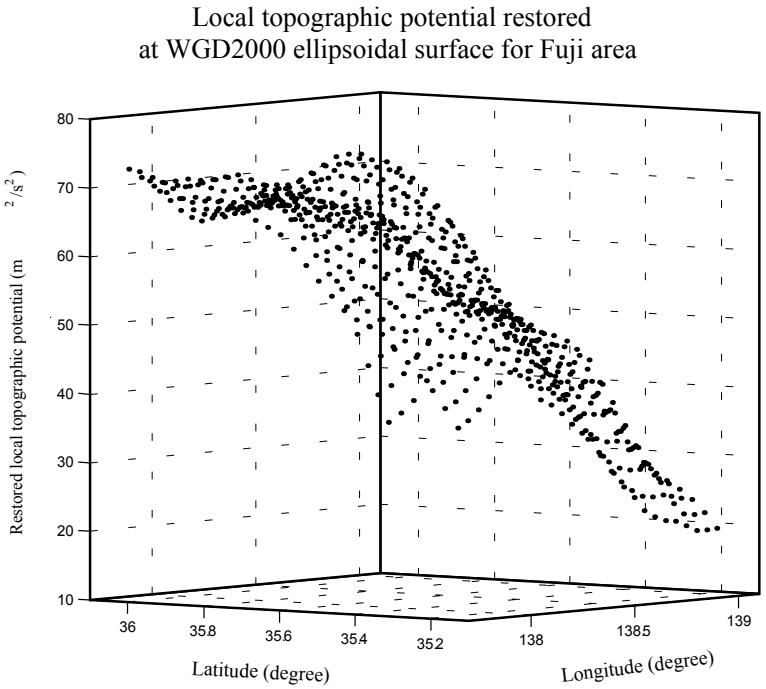

Figure 23: Restored local topographic potential at WGD2000 ellipsoid.

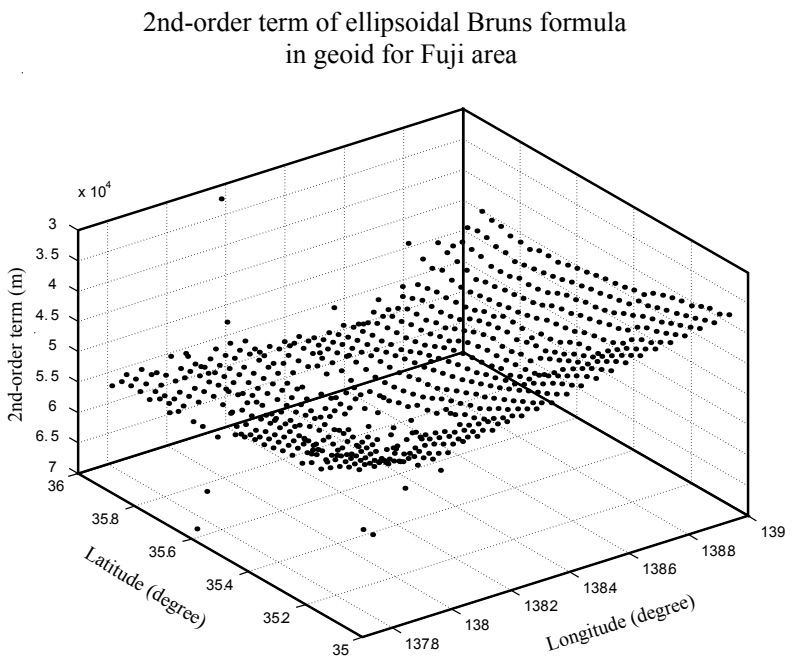

Figure 24: Geographical distribution of second-order term of ellipsoidal Bruns formula in geoid height.

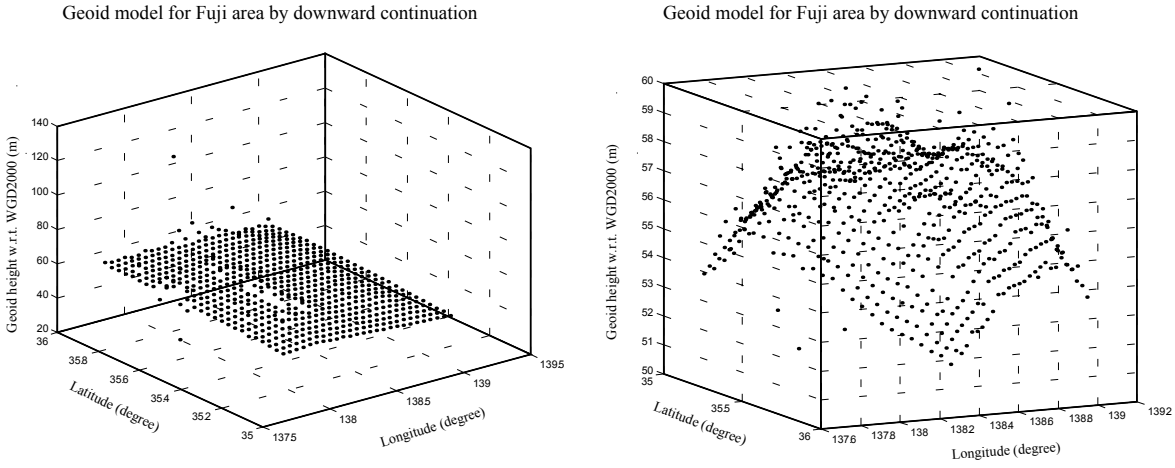

Figure 25: Final geoid model by downward continuation with respect to WGD2000 reference ellipsoid: (a; left) in a smaller scale, and (b; right) in a larger scale.

The second-order term of ellipsoidal Bruns' formula is evaluated for the test data and its geographical distribution is shown in Fig. 24. The term may have a magnitude of an order of 10^{-4} m. On the cm level discussion of the geoid modeling, we can safely ignore this term.

The final geoid model is shown in Fig. 25 (a) on a small scale and in (b) on a large scale. The outliers could yield geoid errors of several tens of meters.

The reference geoid model over Japan, JGEOID2000, matches with GPS/level geoid data on a level of few tens of cm in the area. Then, comparisons with JGEOID2000 reveal

the errors of the geoid model obtained by this study. Fig. 26 shows the geoid differences between the two models against JGEOID2000 geoid height. The geoid model by this study shows significant biases of more than 10 m. Fig. 22 tells us that the biases are coming from the EGM96 contributions. The author is doubtful with the ellipsoidal coefficients over Japan, which were converted from the spherical coefficients of EGM96, because there are no such big deviations in the EGM96 geoid from the GPS/leveling geoid undulations when the author computed it from the original spherical coefficients. Therefore, we will not further evaluate the resulting geoid model.

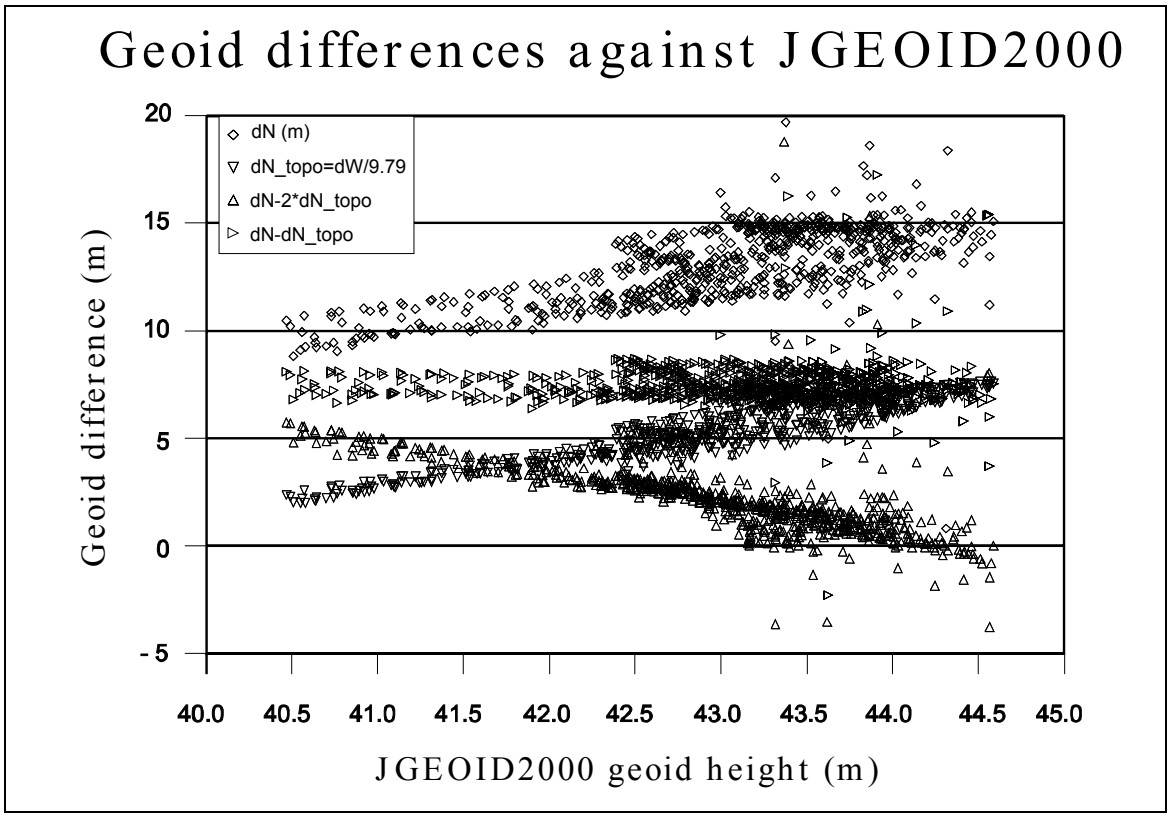

Figure 26: Geoid differences between downward-continued models by the present study and the reference gravimetric geoid model, JGEOID2000 against JGEODI2000 geoid height. Diamonds show the raw differences, vertical triangles are the contributions of local topographic potential at the ellipsoid, triangles show the differences after reversing the sign of the local topographic restoration, and laying triangles show the differences after removing the restoration term due to the local topography at the ellipsoid.

The author computes a geoid model from the same data, with the Tykhonov regularization, which was applied in the case study of Baden-Württemberg by Ardalan (2000). The results show that the regularization cannot constrain the outliers, no significant differences are observed in the resulting models, and that the recovered incremental potentials on the ellipsoid are totally suppressed to some extent. For the densely covered data, the regularization is not necessary or useful in the application.

7 Concluding remarks

The application of downward continuation in mountainous areas is discussed in this study. We propose several corrections and improvement over the previous study by Ardalan (2000). Although the local topographic mass contributions are computed with orthometric heights instead of ellipsoidal heights, the errors do not force major changes in the resulting geoid model except the biases. The resulting model is not completely satisfactory, but the key issues of the application become clear. We must develop some physical reductions to suppress the variations of incremental gravity modulus at the topographic surface. The compensation at Moho and Conrad discontinuities and inclusion of a mass density variation model of the crust should be among such reductions. In the mountainous areas of Japan, the geological structures of the topography are complicated and the densities may vary significantly even in the topographic masses. Especially in volcanic areas thick sediments with lower density cover the topographic surface and the depths of base rocks sometimes are shallower than the zero-height level. Therefore, the density variations in the topography or even in the crust must be considered in order to further the study of the application. In such cases it is desirable that the depths of density discontinuity are determined externally, for example, by seismological study and, that the densities are modeled by fitting to the gravity field.

References

Ardalan AA (2000) High Resolution Regional Geoid Computation in the World Geodetic Datum 2000 – based upon collocation of linearized observational functionals of the type GPS, gravity potential and gravity intensity. Ph.D. Thesis, Department of Geodesy and Geoinformatics, Stuttgart University

Grafarend EW, Ardalan AA (1999) World Geodetic Datum 2000. Journal of Geodesy 73, 611-623

Hagiwara Y (1975) Conventional and spherical Bouguer corrections. Journal of the Geodetic Society of Japan 21, 16-18 (in Japanese with English abstract)

Kuroishi Y (2001b) A new geoid model for Japan, JGEOID2000. In: Sideris M (ed.) Gravity, Geoid and Geodynamics 2000, International Association of Geodesy Symposia Vol 123, Springer, Berlin Heidelberg New York, 329-333

Martinec Z (1998) Boundary-Value Problem for Gravimetric Determination of a Precise Geoid, Lecture Notes in Earth Sciences 73, Springer

Schriftenreihe Institut für Photogrammetrie der Universität Stuttgart, Stuttgart University, Geschwister-Scholl-Str. 24/D, D-70174 Stuttgart
Fax: ++49 711 121 3297; Internet: http://www.ifp.uni-stuttgart.de

---

Nr.	1	(1976)	Vorträge des Lehrgangs Numerische Photogrammetrie (III), Esslingen 1975 - vergriffen
Nr.	2	(1976)	Vorträge der 35. Photogrammetrischen Woche Stuttgart 1975
Nr.	3	(1976)	Contributions of the XIIIth ISP-Congress of the Photogrammetric Institute, Helsinki 1976 - vergriffen
Nr.	4	(1977)	Vorträge der 36. Photogrammetrischen Woche Stuttgart 1977
Nr.	5	(1979)	E. Seeger: Das Orthophotoverfahren in der Architekturphotogrammetrie, Dissertation
Nr.	6	(1980)	Vorträge der 37. Photogrammetrischen Woche Stuttgart 1979
Nr.	7	(1981)	Vorträge des Lehrgangs Numerische Photogrammetrie (IV): Grobe Datenfehler und die Zuverlässigkeit der photogrammetrischen Punktbestimmung, Stuttgart 1980 - vergriffen
Nr.	8	(1982)	Vorträge der 38. Photogrammetrischen Woche Stuttgart 1981
Nr.	9	(1984)	Vorträge der 39. Photogrammetrischen Woche Stuttgart 1983
Nr.	10	(1984)	Contributions to the XVth ISPRS-Congress of the Photogrammetric Institute, Rio de Janeiro 1984
Nr.	11	(1986)	Vorträge der 40. Photogrammetrischen Woche Stuttgart 1985
Nr.	12	(1987)	Vorträge der 41. Photogrammetrischen Woche Stuttgart 1987
Nr.	13	(1989)	Vorträge der 42. Photogrammetrischen Woche Stuttgart 1989
Nr.	14	(1989)	Festschrift - Friedrich Ackermann zum 60. Geburtstag, Stuttgart 1989
Nr.	15	(1991)	Vorträge der 43. Photogrammetrischen Woche Stuttgart 1991
Nr.	16	(1992)	Vorträge zum Workshop "Geoinformationssysteme in der Ausbildung", Stuttgart 1992

Nr.	1	(1987)	K. Eren: Geodetic Network Adjustment Using GPS Triple Difference Observations and a Priori Stochastic Information
Nr.	2	(1987)	F.W.O. Aduol: Detection of Outliers in Geodetic Networks Using Principal Component Analysis and Bias Parameter Estimation
Nr.	3	(1987)	M. Lindlohr: SIMALS; SIMulation, Analysis and Synthesis of General Vector Fields
Nr.	4	(1988)	W. Pachelski, D. Lapucha, K. Budde: GPS-Network Analysis: The Influence of Stochastic Prior Information of Orbital Elements on Ground Station Position Measures
Nr.	5	(1988)	W. Lindlohr: PUMA; Processing of Undifferenced GPS Carrier Beat Phase Measurements and Adjustment Computations
Nr.	6	(1988)	R.A. Snay, A.R. Drew: Supplementing Geodetic Data with Prior Information for Crustal Deformation in the Imperial Valley, California 1988
Nr.	7	(1989)	H.-W. Mikolaiski, P. Braun: Dokumentation der Programme zur Behandlung beliebig langer ganzer Zahlen und Brüche
Nr.	8	(1989)	H.-W. Mikolaiski: Wigner 3j Symbole, berechnet mittels Ganzzahlarithmetik
Nr.	9	(1989)	H.-W. Mikolaiski: Dokumentation der Programme zur Multikplikation nach Kugelfunktionen entwickelter Felder
Nr.	10	(1989)	H.-W. Mikolaiski, P. Braun: Dokumentation der Programme zur Differentiation und zur Lösung des Dirichlet-Problems nach Kugelfunktionen entwickelter Felder
Nr.	11	(1990)	L. Kubácková, L. Kubácek: Elimination Transformation of an Observation Vector preserving Information on the First and Second Order Parameters
Nr.	12	(1990)	L. Kubácková: Locally best Estimators of the Second Order Parameters in Fundamental Replicated Structures with Nuisance Parameters
Nr.	13	(1991)	G. Joos, K. Jörg: Inversion of Two Bivariate Power Series Using Symbolic Formula Manipulation
Nr.	14	(1991)	B. Heck, K. Seitz: Nonlinear Effects in the Scalar Free Geodetic Boundary Value Problem
Nr.	15	(1991)	B. Schaffrin: Generating Robustified Kalman Filters for the Integration of GPS and INS
Nr.	16	(1992)	Z. Martinec: The Role of the Irregularities of the Earth's Topography on the Tidally Induced Elastic Stress Distribution within the Earth
Nr.	17	(1992)	B. Middel: Computation of the Gravitational Potential of Topographic-Isostatic Masses
Nr.	18	(1993)	M.I. Yurkina, M.D. Bondarewa: Einige Probleme der Erdrotationsermittlung
Nr.	19	(1993)	L. Kubácková: Multiepoch Linear Regression Models
Nr.	20	(1993)	O.S. Salychev: Wave and Scalar Estimation Approaches for GPS/INS Integration

Schriftenreihe der Institute des Studiengangs Geodäsie und Geoinformatik (ehemals Fachbereich Vermessungswesen); Technical Reports Department of Geodesy and GeoInformatics, Stuttgart University, Geschwister-Scholl-Str. 24/D, D-70174 Stuttgart
Fax: ++49 711 121 3285; Internet: http://www.uni-stuttgart.de/gi/research

---

Nr. 1994.1	(1994)	H.-J. Euler: Generation of Suitable Coordinate Updates for an Inertial Navigation System
Nr. 1994.2	(1994)	W. Pachelski: Possible Uses of Natural (Barycentric) Coordinates for Positioning
Nr. 1995.1	(1995)	J. Engels, E.W. Grafarend, P. Sorcik: The Gravitational Field of Topographic-Isostatic Masses and the Hypothesis of Mass Condensation - Part I & II
Nr. 1995.2	(1995)	Minutes of the ISPRS Joint Workshop on Integrated Acquisition and Interpretation of Photogrammetric Data
Nr. 1996.1	(1996)	Festschrift für Klaus Linkwitz anläßlich der Abschiedsvorlesung im Wintersemester 1995/96; herausgegeben von Eberhard Baumann, Ulrich Hangleiter und Wolfgang Möhlenbrink
Nr. 1996.2	(1996)	J. Shan: Edge Detection Algorithms in Photogrammetry and Computer Vision
Nr. 1997.1	(1997)	Erste Geodätische Woche Stuttgart, 7.-12. Oktober 1996; herausgegeben von A. Gilbert und E.W. Grafarend
Nr. 1997.2	(1997)	U. Kälberer: Untersuchungen zur flugzeuggetragenen Radaraltimetrie
Nr. 1998.1	(1998)	L. Kubácek, L. Kubácková: Regression Models with a weak Nonlinearity
Nr. 1999.1	(1999)	GIS-Forschung im Studiengang Geodäsie und Geoinformatik der Universität Stuttgart; herausgegeben von M. Sester und F. Krumm
Nr. 1999.2	(1999)	Z. Martinec: Continuum Mechanics for Geophysicists and Geodesists. Part I: Basic Theory
Nr. 1999.3	(1999)	J. H. Dambeck: Diagnose und Therapie geodätischer Trägheitsnavigationssysteme. Modellierung – Systemtheorie – Simulation – Realdatenverarbeitung
Nr. 1999.4	(1999)	G. Fotopoulos, C. Kotsakis, M. G. Sideris: Evaluation of Geoid Models and Their Use in Combined GPS/Levelling/Geoid Height Network Adjustment
Nr. 1999.5	(1999)	Ch. Kotsakis, M. G. Sideris: The Long Road from Deterministic Collocation to Multiresolution Approximation
Nr. 1999.6	(1999)	Quo vadis geodesia...? Festschrift for Erik W. Grafarend on the occasion of his 60th birthday; herausgegeben von F. Krumm und V.S. Schwarze - vergriffen, out of stock -
Nr. 2000.1	(2000)	J. Banks, K. Kubik, Y. H. Lu: Investigation into Digital Image Matching
Nr. 2000.2	(2000)	P. Xu, E. Cannon, G. Lachapelle: Mixed Integer Observation Models, GPS Decorrelation and Integer Programming
Nr. 2000.3	(2000)	B. Voosoghi: Intrinsic Deformation Analysis of the Earth Surface Based on 3-Dimensional Displacement Fields Derived from Space Geodetic Measurements

Nr. 2001.1	(2001)	F. Butsch: Untersuchungen zur elektromagnetischen Interferenz bei GPS
Nr. 2001.2	(2001)	A. M. Abolghasem: Numerical Modeling of Post-Seismic Displacement Fields
Nr. 2002.1	(2002)	J. L. Awange: Gröbner Bases, Multipolynomial Resultants and the Gauss-Jacobi Combinatorial Algorithms - Adjustment of Nonlinear GPS/LPS Observations
Nr. 2002.2	(2002)	Y. Kuroishi: On the Application of Downward Continuation of Surface Gravity onto the Reference Ellipsoid, to the Geoid Determination in Mountainous Areas